12-10-2010

Double compact objects as low-frequency gravitational wave sources

Krzysztof Belczynski

Matthew Benacquista

Tomasz Bulik

Recommended Citation

Krzysztof Belczynski, et. al., (2010) Double compact objects as low-frequency gravitational wave sources.Astrophysical Journal725:1816. DOI: http://doi.org/10.1088/0004-637X/725/1/816

The Astrophysical Journal, 725:816–823, 2010 December 10 doi:10.1088/0004-637X/725/1/816

DOUBLE COMPACT OBJECTS AS LOW-FREQUENCY GRAVITATIONAL WAVE SOURCES

Krzysztof Belczynski[1,2], Matthew Benacquista[2], and Tomasz Bulik[1]
[1] Astronomical Observatory, University of Warsaw, Al. Ujazdowskie 4, 00-478 Warsaw, Poland
[2] Center for Gravitational Wave Astronomy, University of Texas at Brownsville, Brownsville, TX 78520, USA
Received 2008 October 28; accepted 2010 October 12; published 2010 November 19

ABSTRACT

We study the Galactic field population of double compact objects (DCOs; NS–NS, BH–NS, BH–BH binaries) to investigate the number (if any) of these systems that can potentially be detected with the *Laser Interferometer Space Antenna* (*LISA*) at low gravitational wave frequencies. We calculate the Galactic numbers and physical properties of these binaries and show their relative contributions from the disk, bulge, and halo. Although the Galaxy hosts $\sim 10^5$ DCO binaries emitting low-frequency gravitational waves, only a handful of these objects in the disk will be detectable with *LISA*, but none from the halo or bulge. This is because the bulk of these binaries are NS–NS systems with high eccentricities and long orbital periods (weeks/months) causing inefficient signal accumulation (a small number of signal bursts at periastron passage in one year of *LISA* observations) and rendering them undetectable in the majority of these cases. We adopt two evolutionary models that differ in their treatment of the common envelope (CE) phase that is a major (and still mostly unknown) process in the formation of close DCOs. Depending on the evolutionary model adopted, our calculations indicate the likely detection of about four NS–NS binaries and two BH–BH systems (model A; likely survival of progenitors through CE) or only a couple of NS–NS binaries (model B; suppression of the DCO formation due to CE mergers).

Key words: binaries: close – gravitation – stars: evolution – stars: neutron

Online-only material: color figures

1. INTRODUCTION

The *Laser Interferometer Space Antenna* (*LISA*) is a space-based instrument to search for and observe gravitational radiation (GR; e.g., Hughes 2006). A system of three satellites (5 million km apart), orbiting the Sun, will form an interferometer sensitive to low-frequency GR ($\sim 5 \times 10^{-5}$– 1 Hz). The main sources of GR at these low frequencies are in-spirals of supermassive black holes (BHs) in the center of merging galaxies, extreme mass ratio in-spirals (EMRIs) of stellar-mass objects into the supermassive BHs, and nearby (mostly Galactic) compact binaries. Double white dwarf binaries (WD–WD) are the largest population of Galactic systems that are expected to produce a confusion-limited noise in the detector, with several thousand of the louder systems being potentially resolved. A number of studies have concentrated on studies of double white dwarfs in the context of low-frequency *LISA* observations (e.g., Hils et al. 1990; Farmer & Phinney 2003; Nelemans et al. 2004; Ruiter et al. 2009, 2010). Here, we focus on the other, much less studied groups of compact systems; double neutron star binaries (NS–NS), black hole–neutron star (BH–NS), and double black hole (BH–BH) systems. Out of all such double compact objects (DCOs) only a handful of NS–NS have been discovered in radio surveys (e.g., Lorimer 2005). Although much less common than double white dwarfs, DCOs produce much stronger GR signals because they are much denser and more massive than white dwarfs.

Mergers of all types of DCOs are expected to be prime candidates for high-frequency ground-based gravitational wave interferometers such as LIGO or VIRGO, while mergers of NS–NS and BH–NS are proposed as potential progenitors of short–hard gamma-ray bursts (Paczynski 1986). DCOs have been studied extensively over the past 2 decades, bringing new understanding of their formation, particularly in the context of population synthesis studies (e.g., Tutukov & Yungelson 1994; Lipunov et al. 1997; Portegies Zwart & Yungelson 1998; Belczynski & Bulik 1999; Fryer et al. 1999; Bloom et al. 1999; Nelemans at al. 2001; Hurley et al. 2002; Voss & Tauris 2003; Dewi & Pols 2003; Pfahl et al. 2005). Merger rates were recently presented and discussed by Kalogera et al. (2004; empirical estimates) and Belczynski et al. (2010; population synthesis).

In this study, we analyze the field Galactic population (disk, bulge, and halo) of DCOs. We do not consider any dynamical interactions between stars; i.e., evolution of stars in globular clusters is not accounted for and we evolve only field populations. However, we note that despite their relatively small stellar-mass content globular clusters may contribute significantly to the formation of BH–BH binaries (Kulkarni at al. 1993; Gultekin et al. 2004; O'Leary et al. 2006; Sadowski et al. 2008; Downing et al. 2010). On the other hand, the formation of DCOs with NSs was found to be inefficient in globular cluster environments (e.g., Phinney 1991; Grindlay et al 2006; Ivanova et al. 2008). Using population synthesis methods we predict numbers and physical properties of DCOs; we then calculate their spatial distribution and estimate the low-frequency GR signal that may arise from these binaries.

2. MODELING

2.1. Population Synthesis

We have used the population synthesis code `StarTrack` to calculate the numbers and properties of DCOs. The full description of the code can be found in Belczynski et al. (2002, 2008). The code utilizes a set of stellar models (Hurley et al. 2000) that allow for evolution of stars at different metallicities. The compact object formation follows self-consistently from the stellar models, extended to the formation of the FeNi core (Timmes et al. 1996). During the core collapse the fall back and direct BH formation is accounted for (Fryer & Kalogera 2001) and the newly born compact objects receive natal kicks (Hobbs et al. 2005). Formation of low-mass NSs through electron

capture supernovae is also accounted for (e.g., Podsiadlowski et al. 2004). Binary interactions are treated in detail and the various processes were calibrated using either results of detailed evolutionary calculations (e.g., Wellstein et al. 2001 for mass transfer sequences) or specific sets of observations (e.g., Levine et al. 2000 for tidal interactions).

All of our population synthesis calculations implement the standard evolutionary model presented in Belczynski et al. (2008). We employ our standard model to evolve three different Galactic populations: disk, bulge, and halo. The disk is assumed to have a stellar mass of $4.0 \times 10^{10}\,M_{\odot}$, stars have solar metallicity $Z = 0.02$, and we assume the age of the population to be 10 Gyr with constant star formation throughout the disk lifetime (i.e., the star formation rate is $4\,M_{\odot}\,\mathrm{yr}^{-1}$). The bulge is assumed to have a stellar mass of $1.1 \times 10^{10}\,M_{\odot}$, stars also have solar metallicity $Z = 0.02$, and we assume the age of the population to be 10 Gyr with a burst of star formation lasting through the first Gyr of bulge evolution. The halo is assumed to have a stellar mass of $0.1 \times 10^{10}\,M_{\odot}$, the stars have sub-solar metallicity $Z = 0.001$, and we assume the age of the population to be 13 Gyr with a burst star formation at the very beginning of halo evolution.

Belczynski et al. (2007) noted that many progenitors of DCOs evolve through a common envelope phase while a donor star is crossing the Hertzsprung gap. Such a star does not have a well-developed core–envelope structure (e.g., Taam & Sandquist 2000) and once in-spiral in a common envelope is started it may very likely lead to a merger whether there is enough orbital energy to expel the envelope or not. Taking these mergers into account leads to a significant decrease in the formation of close DCOs. To estimate the impact of this uncertainty on the *LISA* signal we perform two calculations. In one (Model A), we allow for survival in the case of a common envelope with a Hertzsprung gap donor (i.e., standard energy balance is tested to check for system survival; Webbink 1984), while in the other (model B), we assume that all such common envelope events lead to a merger aborting further binary evolution and thus depleting the population of DCOs.

2.2. Galactic Model

The binaries are distributed at birth throughout the Galaxy according to stellar density models. We assume that the densities are independent of time. For the bulge, we choose a spherical density with a normal distribution in the radial coordinate and a cutoff radius of 3.5 kpc, so $\rho_b \propto e^{-(r/r_{0b})^2}$, where $r_{0b} = 500$ pc (Nelemans et al. 2004). The disk population is assumed to be axially symmetric with cylindrical radius and vertical height distribution given by a double exponential $\rho_{\rm d} \propto e^{-R/R_{0d}} e^{-|z|/z_{0d}}$, with $R_{0d} = 2.5$ kpc and $z_{0d} = 200$ pc. Finally, we distribute the halo binaries according to a simplistic spherical model with $\rho_{\rm h} \propto (1 + \frac{r}{a_0})^{-3.5}$, with $a_0 = 3.5$ kpc. The disk and bulge systems are given initial rotational velocities in the plane of the disk, and the halo systems are assumed to have circular orbits corresponding to their initial positions. All systems propagate through a Galactic potential and their trajectories change due to the kicks received at the birth of each compact object.

The Galactic gravitational potential is the sum of the bulge, disk, and halo potentials. The disk and bulge are described by the Miyamoto & Nagai (1975) potentials:

$$\Phi(R, z) = \frac{GM_i}{\sqrt{R^2 + (a_i + \sqrt{z^2 + b_i})}}, \quad (1)$$

where $R = \sqrt{x^2 + y^2}$, the index i corresponds to bulge and disk, a_i and b_i are the parameters, and M_i is the mass. The halo potential is assumed to be

$$\Phi(r) = -\frac{GM_h}{r_c}\left[\frac{1}{2}\ln\left(1 + \frac{r^2}{r_2^2}\right) + \frac{r_c}{r}\mathrm{atan}\left(\frac{r}{r_c}\right)\right], \quad (2)$$

where r_c is the core radius, and M_h is the parameter describing the mass of the halo (Paczynski 1990). The mass of such a halo is divergent so we introduce a cutoff radius $r_{\rm cut}$ beyond which the halo density falls to zero, and the potential is $\Phi(r) \propto r^{-1}$. The bulge is described by $M_1 = 1.12 \times 10^{10}\,M_{\odot}$, $a_1 = 0$ kpc, and $b_1 = 0.277$ kpc, and the disk by $M_2 = 8.78 \times 10^{10}\,M_{\odot}$, $a_2 = 4.2$ kpc, and $b_2 = 0.198$ kpc. For the halo potential, we use $r_c = 6.0$ kpc, $r_{\rm cut} = 100$ kpc, and $M_h = 5.0 \times 10^{10}\,M_{\odot}$. We note that the masses of the potentials differ from the masses of the stellar components in Section 2.1 because we include non-stellar matter and dark matter in the potentials.

2.3. LISA Signal Simulator

We calculate the expected signal in *LISA* as the Michelson signal from an equal-arm interferometer using the long-wavelength approximation for frequencies below 3 mHz (Cutler 1998; Benacquista et al. 2004) and the rigid adiabatic approximation (Rubbo et al. 2004) above this frequency. The gravitational waveform for an eccentric binary with angular frequency $\omega = 2\pi/P_{\rm orb}$ is calculated in the quadruple approximation (Peters & Mathews 1963; Peters 1964). We use the specific form given in Pierro et al. (2001). The overall amplitude of the gravitational wave is proportional to

$$h_0 = \frac{2G^{5/3}\omega^{2/3}M_{\rm chirp}^{5/3}}{rc^4}, \quad (3)$$

where r is the luminosity distance from the Earth to the binary. We assign each binary an arbitrary orientation, and so the contribution of each binary to the *LISA* signal is described by 11 parameters. The masses (M_1 and M_2), luminosity distance (r), and orbital frequency ($f_{\rm orb}$) are used to construct the overall amplitude and the relative amplitudes of the harmonics are obtained from the eccentricity (e). The sky location is obtained from the final positions (θ_s and ϕ_s) of the binaries after propagation through the Galactic potential. The arbitrary orientation includes the initial phase (ϕ_0), the argument of the periastron (γ), and the direction angles of the angular momentum vector (θ_l and ϕ_l). We compute the one-year time domain signal for each harmonic in the waveform up to a frequency of 30 mHz. We have not included periastron precession, although this may prove to be important for longer observation times.

For $e = 0$, all the power in the waveform is concentrated at the $n = 2$ harmonic. At non-zero eccentricity, the power in this waveform is spread out over several harmonics of the orbital frequency. If we define $n_{\rm max}(e)$ to be the harmonic with maximum power for eccentricity e, then for $e \gtrsim 0.8$, $n_{\rm max}(e)$ can be approximated by

$$n_{\rm max} \simeq \frac{1.6}{(1-e)^{1.5}}. \quad (4)$$

The factor of 1.6 arises from maximizing $g\,(n, e)$ from Peters & Mathews (1963). Binaries with $f_{\rm orb}$ below the low-frequency limit ($f_{\rm crit}$) for *LISA* sensitivity may still be observable by *LISA* if

Table 1
Number of Double Compact Binaries in the Galaxy[a]

Component	NS–NS	BH–NS	BH–BH
ALL: disk	281091–238245	45075–17729	621812–424501
ALL: bulge	58658–52520	10347–4388	147260–106170
ALL: halo	6351–6342	2845–2776	37681–36373
ALL: total	346100–297107	58267–24893	806753–567044
LISA: disk	92253–58633	4029–371	6903–6
LISA: bulge	12853–8700	382–48	417–0
LISA: halo	298–291	50–39	36–25
LISA: total	105404–67624	4461–458	7356–31

Notes. [a] Numbers are given for two models: Model A and Model B. ALL: all binaries in a given category. *LISA*: binaries with orbital periods and eccentricities that are likely to contribute to a GR signal in the *LISA* frequency band.

$n_{\max} f_{\rm orb} > f_{\rm crit}$. We use the following approximate criterion to separate potential *LISA* sources from the entire DCO population:

$$P_{\rm orb} < 1.6(1-e)^{-1.5} f_{\rm crit}^{-1}, \quad (5)$$

where $f_{\rm crit} = 5 \times 10^{-5}$ Hz.

LISA instrument noise is simulated by assuming that the power spectral density of the noise is made up of position (or shot) noise ($S_{\rm np}$) and an acceleration noise ($S_{\rm na}$) (converted to strain) given by Cornish (2001). These separate components are combined according to

$$S_{\rm n} = 4S_{\rm np} + 8S_{\rm na}(1+\cos^2(f/f_*)), \quad (6)$$

where $f_* = c/2\pi L$ with the armlength of *LISA* taken to be $L = 5 \times 10^9$ m. We roll off the acceleration below $f_{\rm crit}$, so that $S_{\rm na}(f \leqslant f_{\rm crit}) = S_{\rm na}(f_{\rm crit})$. In reality, the *LISA* noise will probably not follow this simple power law all the way down to our choice of $f_{\rm crit}$, but will begin to rise at a higher frequency.

3. RESULTS

3.1. Physical Properties and Numbers: Model A

In Table 1, we present the number of DCOs predicted for the present time in our Galaxy. Additionally, we list the number of potential *LISA* systems that satisfy Equation (5) and may produce a GR signal in the frequency band of *LISA*. Note that the Galactic population of DCOs is dominated by disk (78%) and bulge (18%) systems with a small contribution of halo binaries (4%). This reflects the fact that the number of DCOs is proportional (for a given evolutionary model) to the stellar mass. Within the entire DCO population, BH–BH systems are dominant (67%), with a significant contribution of NS–NS binaries (28%), and a very small fraction of BH–NS systems (5%). The dominance of BH–BH systems is a consequence of the natal kick model employed, i.e., NSs are given full kicks, while BHs (due to formation through either partial fall back or direct stellar collapse) receive smaller or no natal kicks at all.

The population of potential *LISA* sources is quite different to the entire DCO population. These are the binaries that were formed at close orbits ($P_{\rm orb} \lesssim 150$ days), and constitute only a small fraction of the entire population. The NS–NS *LISA* binaries are 31% of the entire Galactic NS–NS population, while the percentages are 8% for BH–NS and only 1% for BH–BH *LISA* binaries. The decreasing contribution to the *LISA* population is due to the fact that many more BH–BH systems are allowed to form on rather wide orbits while wide NS–NS binaries are mostly disrupted by natal kicks. The bias toward disk binaries is even more pronounced for the *LISA* binaries, in that they mostly originate from the disk (88%), with a significant contribution from the bulge (11.7%) and a negligible number of systems in the halo (0.3%). The increased disk contribution is an effect of star formation history. Basically, the *LISA* group consists of close binaries that can merge (and disappear from the population) in less than the age of the Galaxy. Since the disk is forming stars in an approximately constant manner there is a constant supply of close binaries, while for the bulge and halo, that have formed all the stars ∼10 Gyr ago, many close binaries have already merged. The most striking feature of the *LISA* population is that it mostly consists of NS–NS binaries (90%), with only minor contributions from BH–NS (4%) and BH–BH (6%) systems. For single star evolution with the adopted initial mass function it is predicted that NSs outnumber BHs by about a factor of 5. Binary evolution further affects the numbers. NS–NS progenitors are more likely to avoid mergers in RLOF episodes as the two stars in the binary are close in mass, while for BH–BH progenitors it is likely that dynamical instability develops and a progenitor system enters a common envelope that may lead to a merger.

In Figure 1, we show the characteristic properties of potential *LISA* DCOs. The orbital frequency ($f_{\rm orb} = 1/P_{\rm orb}$) distributions are similar for all types of DCOs and they span a wide range: $f_{\rm orb} \sim 10^{-3}$–10^{-7} Hz ($P_{\rm orb} \sim 0.02$–150 days) and peak at $f_{\rm orb} \sim 5 \times 10^{-5}$ Hz ($P_{\rm orb} \sim 0.5$ days). For frequencies lower than $f_{\rm crit} = 5 \times 10^{-5}$ Hz, the number of systems drops since the eccentricity of a given system needs to increase with decreasing frequency in order for the system to be detectable (see Equation (5)). However, the number of systems with higher eccentricities is gradually decreasing; for high frequencies ($f_{\rm orb} > f_{\rm crit}$) the systems are so tight ($P_{\rm orb} \lesssim 0.5$ days) that the orbital decay is very fast (GR emission) and systems merge causing a depletion in number with increasing frequency. The eccentricity distributions are rather flat for all DCOs. For NS–NS and BH–NS binaries the distributions are slightly skewed toward the high e-values, while the opposite is true for BH–BH systems. The eccentricity distribution is the direct result of the second supernova asymmetry. Since systems with NSs receive, on average, a larger second kick, the NS–NS and BH–NS binaries are more eccentric than BH–BH systems. The rather high fraction (∼40%) of BH–BH systems with small eccentricities ($e < 0.2$) is either the result of direct collapse of a star to a BH or significant fall back of material during the second supernova explosion.

Chirp mass distributions are very different for the three subclasses. The NS–NS chirp mass distribution peaks at $M_{\rm chirp} \sim 1.2\,M_\odot$ with a tail that extends to $M_{\rm chirp} \sim 2\,M_\odot$. Systems with BHs have much flatter distributions but spanning a wide range of chirp masses: $M_{\rm chirp} \sim 1.5$–$4\,M_\odot$ for BH–NS and $M_{\rm chirp} \sim 2.5$–$9\,M_\odot$ for BH–BH binaries. For BH–NS/BH–BH systems the distributions are mostly shaped by the mass distribution of BHs. The lowest mass BHs are found just over $2.5\,M_\odot$ (the adopted maximum NS mass) and they can be as massive as $\sim 15\,M_\odot$ for disk and bulge (high metallicity) while they can reach even higher masses $\sim 30\,M_\odot$ for halo population (low metallicity). Stellar-mass BHs are found in our Galaxy with masses up to $\sim 15\,M_\odot$ (e.g., Ziolkowski 2010), while in the galaxy IC-10 with low-metallicity stars a BH was found with mass ∼24–33 $M_\odot$ (e.g., Prestwich et al. 2007). Note that although we predict such high mass BHs in the halo of our Galaxy there are very few of them, and they do not have very

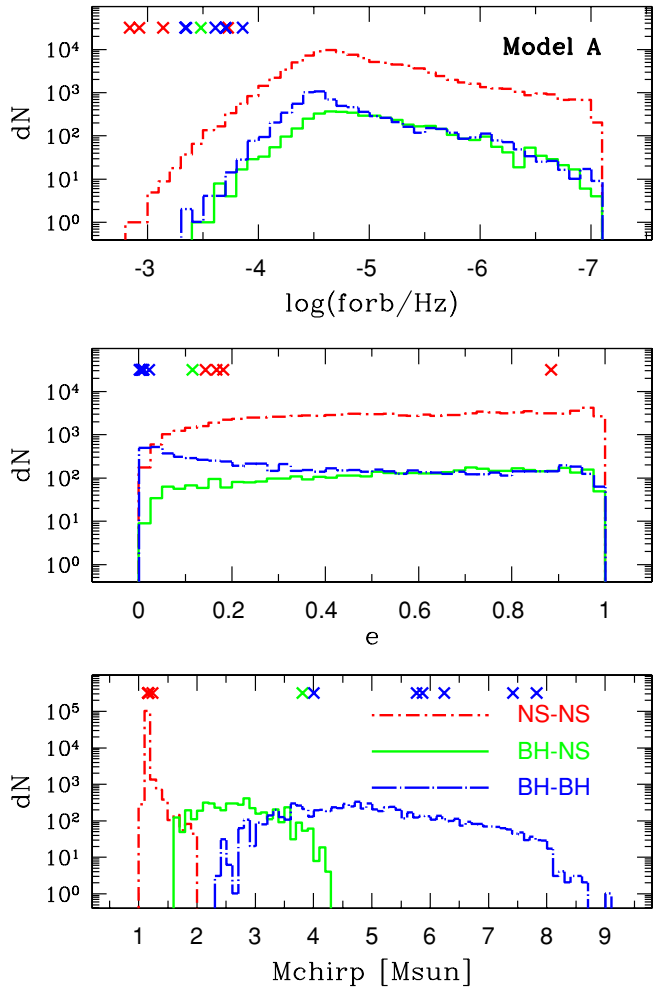

Figure 1. Potential *LISA* Galactic population of DCOs (Model A). The top panel shows the distribution of orbital frequency, the middle panel the distribution of eccentricities, while the bottom panel shows the distribution of chirp masses. Note the dominance of NS–NS binaries. At the top of each panel, we show Galactic resolved DCOs for the most optimistic realization in our calculations (realization 2: Table 2). Since this population is very small (four NS–NS, one BH–NS and six BH–BH binaries), we show all individual resolved sources.

(A color version of this figure is available in the online journal.)

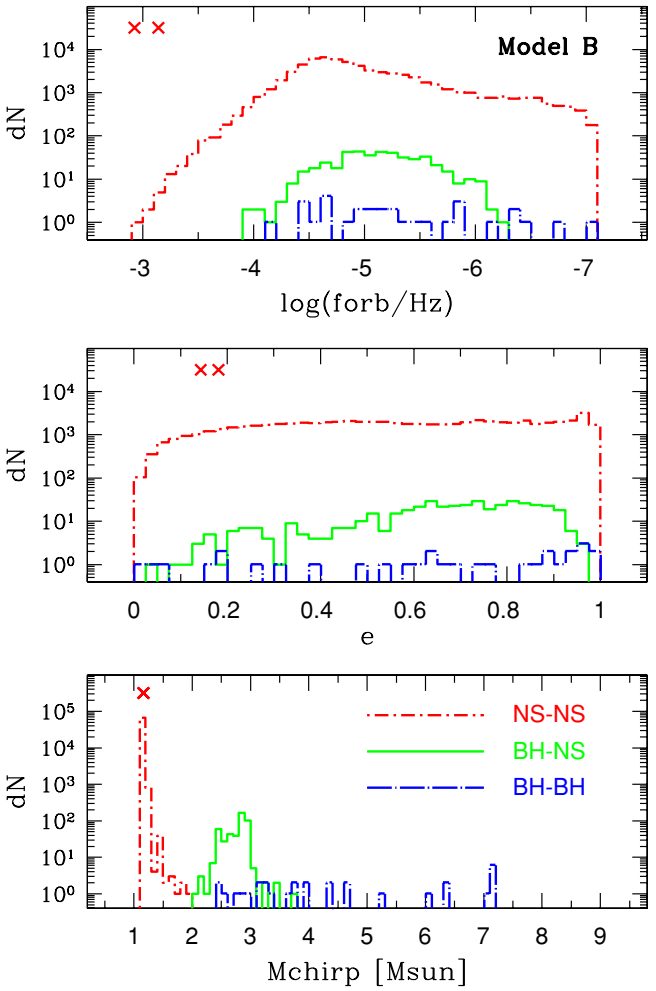

Figure 2. Same as Figure 1 but for model B. The NS–NS dominance is even more pronounced in this model. Note that there are only two resolved sources and they are both NS–NS binaries.

(A color version of this figure is available in the online journal.)

massive companions as the highest chirp masses for BH–BH binaries are $M_{\rm chirp} < 10\,M_{\odot}$. The system in IC-10 is predicted to form a BH–BH binary with $M_{\rm chirp} \sim 20\,M_{\odot}$ and a rather short coalescence time ∼2–3 Gyr (Bulik et al. 2008). Therefore, if such a system has formed in the halo of our Galaxy it has most probably merged by now.

3.2. Physical Properties and Numbers: Model B

For model B, the most affected systems are BH–NS systems (reduction by a factor of ∼2) and BH–BH binaries (reduction by ∼1.4) while NS–NS binaries are affected the least (reduction by ∼1.2). All these changes are not very large, especially in the light of the limited prospects for detecting the majority of these binaries: the majority of these systems are too wide to ever make it to the *LISA* frequency range or to merge within a Hubble time to be detected by ground-based detectors such as LIGO or VIRGO.

For *LISA* binaries, the differences are much more pronounced. BH–BH binaries are reduced by a factor of ∼250, BH–NS by ∼10, and NS–NS by ∼1.5. The progenitors of close *LISA* binaries are subject to one or more common envelope events and thus they are greatly affected in this model. In particular, progenitors of binaries with BHs that start their evolution with stars of rather unequal masses are subject to evolving through the common envelope and merging. Basically, it is predicted that if there is no survival in a common envelope with Hertzsprung gap donors, then there are almost no BH–BH and BH–NS binaries in our Galaxy within the *LISA* frequency band. In this case, only close NS–NS binaries would have a chance to show up in the *LISA* data stream. Although the number of potential *LISA* NS–NS binaries is reduced, it is still quite significant ($\sim 7 \times 10^4$). The physical properties of *LISA* NS–NS binaries in Model B are shown in Figure 2 and are not much different from Model A.

3.3. Spatial Distribution

We present the cumulative distribution (after propagation) of distances of DCOs from the Earth in Figure 3. Halo binaries are born far from the Galactic center and their potential energies are large; the kick velocities may increase them above zero and unbind some of them. Bulge binaries have low potential energies and adding the kick velocities unbinds only a small fraction of them. Their angular momenta are not large since they are all born close to the Galactic center. Thus they remain concentrated in the bulge. Potential energies of disk binaries have a wide

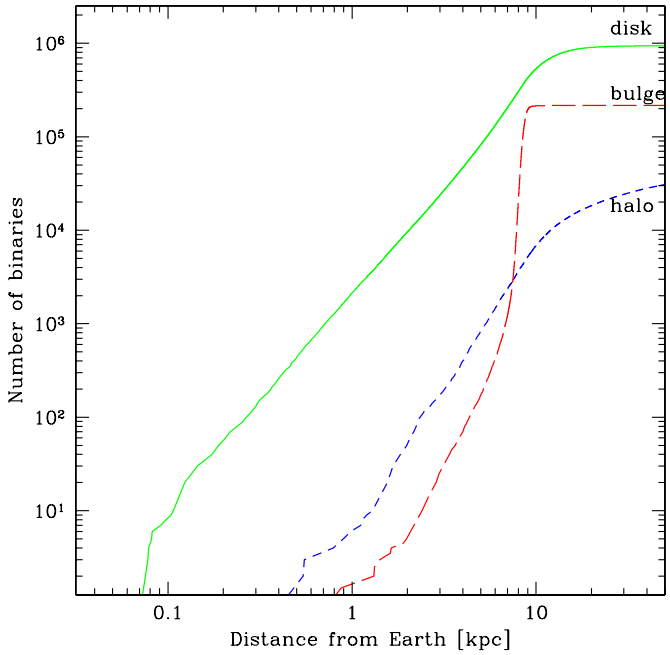

Figure 3. Cumulative distribution of the current distances of simulated binaries from the Earth (model A). The distances are obtained after propagation in the Galactic potential; the binaries have spread out from their birth sites due to natal kicks. We show the three Galactic components separately. Note that the Galactic center is at a distance of ∼8 kpc from Earth.

(A color version of this figure is available in the online journal.)

distribution, depending on the distance from the Galactic center; however, the disk itself is a potential well. The addition of kick velocities increases the potential energy. The angular momenta of the disk binaries on their Galactic orbits are initially aligned perpendicularly to the disk plane, yet after the propagation the kick velocities tend to partially isotropize them. Thus, they form a disk with scale height of ≈0.2 kpc and a radius of ≈15 kpc. The distribution as seen from the Earth initially probes this disk for small distances and the number of DCOs increases with the cube of distance, yet this dependence is only seen for the closest few tens of binaries. For distances from a few hundred parsecs to ≈10 kpc the number of DCOs increases roughly as the distance squared because a flat distribution of sources is probed. For larger distances ($\gtrsim$15 kpc) the dependence flattens out because we reach the end of the disk. The disk binaries are the most likely potential *LISA* sources for the entire distance range in the Galaxy.

3.4. Gravitational Radiation Signature

The gravitational wave signature for a one-year observation has been calculated for each of 10 realizations of both models. Each realization was obtained by redistributing the initial positions of the DCOs according to the stellar density distributions described in Section 2.2. The population has been separated into the different binary types in Figure 4 and compared with a realization of the *LISA* noise. In Figure 5, we separate out the different components of the Galaxy. From this, we see that in both models the disk binaries are the only ones to rise above the *LISA* noise.

We are interested in determining if *LISA* observations can distinguish between these two models. Although we do not have an algorithm for identifying eccentric stellar-mass compact object binaries in the *LISA* data stream, we can still approximate the outcome of such an algorithm. It is possible that the coherent signals from the many harmonics of eccentric binaries can be summed to boost a signal above the *LISA* noise even though each individual harmonic lies buried in the noise (Benacquista 2001, 2002; Larson & Hellings 2009). We assume that some sort of matched filter will be used, and so we can describe the detection statistic as the signal-to-noise ratio (ρ) defined as (Wainstein & Zubakov 1962) $\rho^2 = 4\int_0^\infty [|\tilde{h}(f)h(f)|/S_n(f)]df$, where $S_n(f)$ is the one-sided noise power spectral density. For the purposes of calculating the detection statistic, we use the discrete analog

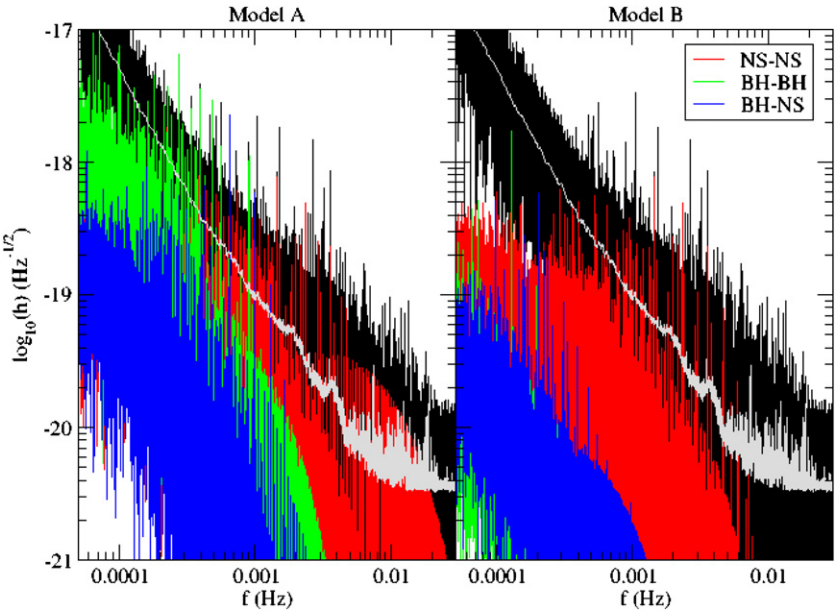

Figure 4. Strain spectral densities of the DCO binaries separated by binary type and compared with the full spectrum containing the DCOs, the WD–WD signal, and the *LISA* noise. The line is a running median over the full spectrum. The left panel shows model A and the right panel shows model B. Note the strong suppression of the BH–BH binaries in model B, and the absence of any detectable signals below ∼0.4 mHz.

(A color version of this figure is available in the online journal.)

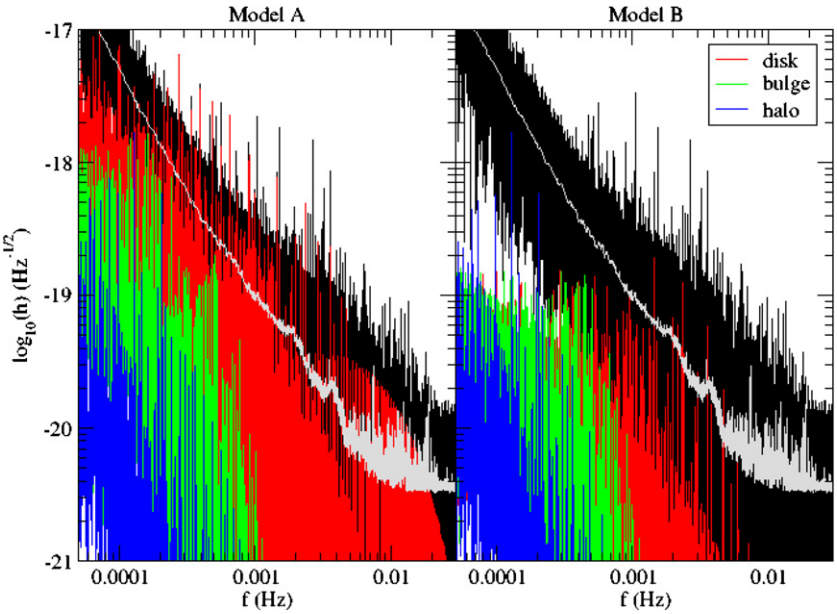

Figure 5. Strain spectral densities of the DCO binaries separated by Galaxy component and compared with the full spectrum containing the DCOs, the WD–WD signal, and the *LISA* noise. The line is a running median over the full spectrum. The left panel shows model A and the right panel shows model B. Note the dominance of the disk binaries in both models, but the significant absence of low-frequency binaries in model B.

(A color version of this figure is available in the online journal.)

of the signal-to-noise ratio given by Schutz (1997):

$$\rho^2 = \sum_{k=0}^{N-1} \frac{||\tilde{h}_k|^2}{S_k} \tag{7}$$

and take S_k to be the running median over 1000 bins of the power spectrum of the *LISA* noise given by Equation (6) combined with a total Galactic white dwarf binary population generated using `StarTrack` (Ruiter et al. 2009, 2010) and the DCO population considered in this work. We calculate $\tilde{h}_k$ for each DCO binary using the *LISA* signal simulator described in Section 2.3.

The foreground noise due to galactic white dwarf binaries is not Gaussian (Timpano et al. 2006). Racine & Cutler (2007) have studied the impact that the non-Gaussianity of the WD–WD foreground has on the detection of EMRIs and supermassive black hole in-spirals (SMBHs). Their conclusion is that the threshold criterion is essentially unchanged after the loudest white dwarf binary signals have been removed from the foreground signals.

Finally, we note that the imposition of a threshold signal-to-noise ratio calculated according to Equation (7) can result in detection of binaries for which no individual harmonic has a signal-to-noise ratio above 1. Matched filtering algorithms have already been demonstrated that can successfully detect SMBH signals within mock *LISA* data (Babak et al. 2008) even though the signal never exceeds the instrument and white dwarf binary confusion noise at any frequency (see Figure 1 of Arnaud et al. 2007).

We impose a threshold of $\rho \geqslant 10$ in at least one *LISA* channel as the criterion for detection. We find that the number of resolvable DCO binaries ranges from 3 to 11 in model A and from 0 to 4 in model B. The bulk of the potentially detectable very low-frequency sources in model A are BH–BH binaries that are dramatically suppressed in model B. This is borne out by the estimates of resolvable binaries where the number of resolvable BH–BH binaries drops to zero in model B. Thus, detection of high-mass, low-frequency binaries can be used to distinguish between these two models. In model A, there is a relatively large number of BH–BH binaries at low frequencies: at 10^{-4} Hz there is 1 BH–BH for each 10 NS–NS (Figure 1), while there is only 1 BH–BH for each 500 NS–NS in model B (Figure 2). Since at these frequencies binaries have relatively large orbital separations, neutron stars that are of much lower mass than black holes do not generate a detectable GR signal, while massive black hole systems do. For lower frequencies ($\lesssim 10^{-5}$ Hz) corresponding to yet larger orbital separations, even the most massive BH–BH binaries do not generate detectable signal, although they dominate over other DCOs. The distribution of the potentially resolvable binaries for each realization is presented in Table 2.

4. SUMMARY

We have calculated, in a self-consistent way, the GR signal of Galactic DCOs and found that several DCOs can be detected and resolved in a one-year observation with an instrument like *LISA*. In model A, we find comparable numbers of BH–BH and NS–NS binaries, while no BH–BH binaries are observed in model B. Such an observation would shed new light on DCO studies as at present we have only detected nine NS–NS systems. DCOs with a BH are yet to be discovered. *LISA* could potentially detect several of these binaries. Starting with NS–NS systems, these potential detections could answer a number of questions. Do nearly all NS–NS systems host low-mass NSs ($\sim 1.35\,M_\odot$) as seems to happen in a known sample discovered through radio-pulsar surveys or is this only some observational bias? Galactic merger rates appear consistent with the notion that NS–NS are short GRB progenitors. But would this be confirmed by a sample detected by *LISA*? Detection of any DCOs with BHs would be a feat in and of itself. Although a number of these systems are expected from evolutionary calculations, these are usually burdened with rather large uncertainties. Detections of BH–BH binaries would provide very valuable tests for evolutionary

Table 2
Distribution of Resolvable Double Compact Binaries in the Galaxy[a]

Realization	Model A			Model B		
	BH–BH	BH–NS	NS–NS	BH–BH	BH–NS	NS–NS
0	3	0	5	0	0	1
1	2	0	4	0	0	1
2	6	1	4	0	0	2
3	2	0	4	0	0	1
4	1	1	5	0	0	3
5	1	0	2	0	0	0
6	1	0	6	0	0	2
7	2	0	2	0	0	0
8	3	0	3	0	0	2
9	2	0	5	0	0	4
	2.3 ± 1.5	0.2 ± 0.4	4 ± 1.3	0	0	1.7 ± 1.3
Total		6.5 ± 2.2			1.7 ± 1.3	

Notes. [a] These numbers represent a conservative estimate as our population synthesis model assumes a stellar disk content of $\sim 4 \times 10^{10}\,M_{\odot}$, while our dynamical calculations use a disk mass content of $\sim 8 \times 10^{10}\,M_{\odot}$. The gas fraction of the disk is around 25% (Naab & Ostriker 2006), leaving the remaining $\sim 2 \times 10^{10}\,M_{\odot}$ as dark matter. If the dark matter content of the disk is not this high, then we have underestimated the stellar content of the disk. At most, these numbers could be 50% higher if there is no dark matter content to the disk.

codes that are used in a number of studies. Knowledge of BH numbers and their basic properties can put direct constraints on the evolution of their progenitors—the most massive stars. In particular, one such example was presented in our study. Depending on a common envelope model, the number of BH–BH systems that could be detected with *LISA* vanishes. So just by their presence (or lack of thereof) in the signal one could test an evolutionary phase that is virtually undetectable due to its shortness ($\sim 10^3$–10^4 yr). And it is interesting to note that although the common envelope was proposed more than 30 years ago (Paczynski 1976), there is still a surprising lack of understanding of the outcome—and the outcome is crucial for the formation of Type Ia supernova progenitors (close white dwarf binaries) or any type of X-ray binaries that are currently observed even in external galaxies by *Chandra* or *XMM*, just to name a few examples. Although DCOs will most likely be discovered first in GR with advanced ground-based interferometers (e.g., LIGO, VIRGO), they will be detected only in the in-spiral and merger phases, preventing a measurement of their orbital parameters (e.g., separations and eccentricities). Additionally, the merger rates are too small to expect detections in the Galaxy, so *LISA* can provide a small but unique sample of Galactic DCOs.

The number of detectable compact object binaries that we found in this analysis is somewhat smaller than the 42 detectable systems predicted by Nelemans et al. (2001). However, this can be reasonably explained by the differences in the overall population numbers between the two simulations. The total number of compact object binaries predicted in our simulation ranges between 0.9×10^6 for model B and 1.2×10^6 for model A, while Nelemans et al. predict 4.0×10^6 such systems. Thus, our prediction of ~ 11 systems is comparable with Nelemans et al. It should be noted, however, that our estimate is conservative as we have assumed no prior removal of any WD–WD signals from the calculated value of S_k, and we have assumed an observation time of 1 year. In reality, we expect some removal of the loud WD–WD signals and the nominal mission lifetime of *LISA* is three years. On the other hand, we have not included any penalties incurred by the larger parameter space needed for the analysis of eccentric systems.

We thank Joe Romano, Ashley Ruiter, and two referees for a number of helpful comments. The authors acknowledge the hospitality of the Aspen Center for Physics and support from MSHE grants N N203 302835 (T.B., K.B.) and N N203 404939 (K.B.), and NASA grants NNX08AB74G (M.J.B.) and NNX09AV06A to the Center for Gravitational Wave Astronomy, UTB (K.B., M.J.B).

REFERENCES

Arnaud, K., et al. 2007, Class. Quantum Grav., 24, S551
Babak, S., et al. 2008, Class. Quantum Grav., 25, 114037
Belczynski, K., & Bulik, T. 1999, A&A, 346, 91
Belczynski, K., Kalogera, V., & Bulik, T. 2002, ApJ, 572, 407
Belczynski, K., Taam, R., Kalogera, V., Rasio, F., & Bulik, T. 2007, ApJ, 662, 504
Belczynski, K., et al. 2008, ApJS, 174, 223
Belczynski, K., et al. 2010, ApJ, 715, L138
Benacquista, M. 2001, in AIP Conf. Proc. 586, Relativistic Astrophysics: 20th Texas Symposium, ed. J. C. Wheeler & H. Martel (Melville, NY: AIP), 793
Benacquista, M. 2002, Class. Quantum Grav., 19, 1297
Benacquista, M., DeGoes, J., & Lunder, D. 2004, Class. Quantum Grav., 21, 509
Bloom, J., Sigurdsson, S., & Pols, O. 1999, MNRAS, 305, 763
Bulik, T., Belczynski, K., & Prestwich, A. 2008, ApJ, submitted (arXiv: 0803.3516)
Cornish, N. J. 2001, Phys. Rev. D, 65, 022004
Cutler, C. 1998, Phys. Rev.D, 57, 7089
Dewi, J. D. M., & Pols, O. R. 2003, MNRAS, 344, 629
Downing, J. M. B., Benacquista, M. J, Giersz, M., & Spurzem, R. 2010, MNRAS, 407, 1946
Farmer, A. J., & Phinney, E. S. 2003, MNRAS, 346, 1197
Fryer, C., & Kalogera, V. 2001, ApJ, 554, 548
Fryer, C., Woosley, S., & Hartmann, D. 1999, ApJ, 526, 152
Grindlay, J., Portegies Zwart, S., & McMillan, S. 2006, Nature, 2, 116
Gultekin, K., Miller, M., & Hamilton, D. 2004, ApJ, 616, 221
Hils, D., Bender, P. L., & Webbink, R. F. 1990, ApJ, 360, 75
Hobbs, G., Lorimer, D. R., Lyne, A. G., & Kramer, M. 2005, MNRAS, 360, 974
Hughes, S. 2006, in AIP Conf. Proc. 873, Laser Interferometer Space Antenna: 6th International LISA Symp., ed. S. M. Merkovitz & J. C. Livas (Melville, NY: AIP), 13
Hurley, J. R., Pols, O. R., & Tout, C. A. 2000, MNRAS, 315, 543
Hurley, J. R., Tout, C. A., & Pols, O. R. 2002, MNRAS, 329, 897
Ivanova, N., Heinke, C., Rasio, F., Belczynski, K., & Fregeau, J. 2008, MNRAS, 386, 553
Kalogera, V., et al. 2004, ApJ, 601, L179
Kulkarni, S., Hut, P., & McMillan, S. 1993, Nature, 364, 421

Larson, S., & Hellings, R. 2009, BAAS, 41, 340
Levine, A., Rappaport, S. A., & Zojcheski, G. 2000, ApJ, 541, L194
Lipunov, V., Postnov, K., & Prokhorov, M. 1997, MNRAS, 288, 245
Lorimer, D. 2005, Living Rev. Rel., 8, 7
Miyamoto, M., & Nagai, R. 1975, PASJ, 27, 533
Naab, T., & Ostriker, J. P. 2006, MNRAS, 366, 899
Nelemans, G., Yungelson, L., & Portegies Zwart, S. 2001, A&A, 375, 890
Nelemans, G., Yungelson, L., & Portegies Zwart, S. 2004, MNRAS, 349, 181
O'Leary, R. M., Rasio, F. A., Fregeau, J. M., Ivanova, N., & O'Shaughnessy, R. 2006, ApJ, 637, 937
Paczynski, B. 1976, in IAU Symp. 73, Structure and Evolution of Close Binary Systems, ed. P. Eggleton et al. (Cambridge: Cambridge Univ. Press), 75
Paczynski, B. 1986, ApJ, 308, L43
Paczynski, B. 1990, ApJ, 348, 485
Peters, P. 1964, Phys. Rev., 136, 1224
Peters, P., & Mathews, J. 1963, Phys. Rev., 131, 434
Pfahl, E., Podsiadlowski, P., & Rappaport, S. 2005, ApJ, 628, 343
Phinney, S. 1991, ApJ, 380, L17
Pierro, V., Pinto, I., Spallicci, A., Laserra, E., & Recano, F. 2001, MNRAS, 325, 358
Podsiadlowski, P., et al. 2004, ApJ, 612, 1044
Portegies Zwart, S., & Yungelson, L. 1998, A&A, 332, 173
Prestwich, A., et al. 2007, ApJ, 669, L21
Racine, E., & Cutler, C. 2007, Phys. Rev. D, 76, 124033
Rubbo, L., Cornish, N., & Poujade, O. 2004, Phys. Rev. D, 69, 082003
Ruiter, A., Belczynski, K., Benacquista, M., & Holley-Bockelmann, K. 2009, ApJ, 693, 383
Ruiter, A., Belczynski, K., Benacquista, M., Larson, S., & Williams, G. 2010, ApJ, 717, 1006
Sadowski, A., et al. 2008, ApJ, 676, 1162
Schutz, B. 1997, in Fundamental Physics in Space, ed. A. Wilson (ESA SP-420; Noordwijk: ESA), 265
Taam, R. E., & Sandquist, E. L. 2000, ARA&A, 38, 113
Timmes, F. X., Woosley, S. E., & Weaver, T. A. 1996, ApJ, 457, 834
Timpano, S. E., Rubbo, L. J., & Cornish, N. J. 2006, Phys. Rev. D, 73, 122001
Tutukov, A., & Yungelson, L. 1994, MNRAS, 268, 871
Voss, R., & Tauris, T. 2003, MNRAS, 342, 1169
Wainstein, L. A., & Zubakov, V. D. 1962, Extraction of Signals from Noise (Englewood Cliffs, NJ: Prentice-Hall)
Webbink, R. 1984, ApJ, 277, 355
Wellstein, S., Langer, N., & Braun, H. 2001, A&A, 369, 939
Ziolkowski, J. 2010, Mem. Soc. Astron. Ital., 81, 294